Nigerian Journal of Engineering Science Research (NIJESR).
Vol. 6, Issue 2, pp.01-11, June, 2023

ISSN: 2636-7114
Journal Homepage: https://www.iuokada.edu.ng/journals/nijesr/

Numerical and Computational Based Models for Modelling the Effect of the Spatter Index in Mild Steel TIG Welding Process

[1a]Amadhe F. O, [1b]Achebo J. I., [2c]Obahiagbon K., *[1d]Ozigagun A

[1]Department of Production Engineering, University of Benin, Benin City, Nigeria.

[a]francisoghenerurie@gmail.com; [b]joseph.achebo@uniben.edu; [d]andrewzigs@yahoo.com

[2]Department of Chemical Engineering, University of Benin, Benin City, Nigeria.

[c]kess.obahiagbon@uniben.edu

**Corresponding Author: Ozigagun A.; andrewzigs@yahoo.com*

Manuscript History
Received: 30/04/2023
Revised: 18/06/2023
Accepted: 25/06/2023
Published: 30/06/2023

Abstract: *The welding process is an important process that involves the use of heat, pressure, or a combination of both to join materials that may be similar or dissimilar. Manufacturing industries generally rates the Tungsten Inert Gas (TIG) good due to its conservation of energy during use. However, there are common challenges associated with the TIG process, which are spattering, cold laps, cold shut, shallow penetration, porosity, cracking, insufficient strength. The aim of current study is to use the Response Surface Methodology (RSM) and Artificial Neural Network (ANN) to optimize and find out and the value effects of the Spatter Index formed using TIG welding parameters on mild steel. The input variables for the statistical design of experiments (DOEs) were weld current, weld voltage, and gas flowrate. These variables were entered into Design Expert 7.01 software to create a DOE for 20 experimental runs. The output parameter, which was the Spatter Index, was predicted and optimized using the results from these experimental runs. By utilizing the Artificial Neural Network (ANN) optimization method, one of the 30 welding runs was determined to be optimal. The same 20 variables that were predicted were then tested using TIG welding, and the results showed that the predicted values were in close agreement with the experimental values. A numerical optimal solution was produced by the RSM model, which included the following values: 200.72 A current, 20 V voltage, 2.40 mm wire diameter, and 20 m/s wire feed speed. This solution resulted in a weld spatter index of 0.0416173, and it was deemed the best option with a desirability value of 93.9% according to the Design Expert software. The ANN method utilized 15% of the data for validation, 15% for real testing, and the remaining 70% for training purposes. From the results obtained a regression plot which visually displays the correlation between the input variables and the target variable was produced with R2 values of 0.93908. As a result of this, Artificial Neural Network has been identified as the superior prediction model compared to Response Surface Methodology, the ANN output fits closer to the experimental than that of RSM. Thus, the approaches effectively optimized and predicted the weld spatter index.*

Keywords: *Cloud Computing, Adoption of Technology, Diffusion of Innovation, Technology Organization and Environment, Higher Educational Institutions*

INTRODUCTION

Tungsten inert gas (TIG) welding was invented by scientist Russell in 1942, and subsequent research has expanded its application to aluminum-based magnesium alloys (Bhanu, 2022). While various welding methods have been utilized in different industries over the years (Raja, 2023), the TIG technique is a popular choice for joining both non-ferrous and ferrous materials (Yogeshwaran, 2015). TIG welding is a process that utilizes an electric arc and tungsten electrodes to generate heat and fuse dissimilar metals (Natrayan and Kumar, 2019). To promote heat transfer to the workpiece and prevent cathode ablation, tungsten is commonly used as the cathode, while the workpiece serves as the anode. However, increasing welding speed and current to enhance fabrication output can result in weld flaws such as undercutting and humping (Wang, 2019). Fig. 1A shows a TIG welder while Fig. 1B shows weld defects.

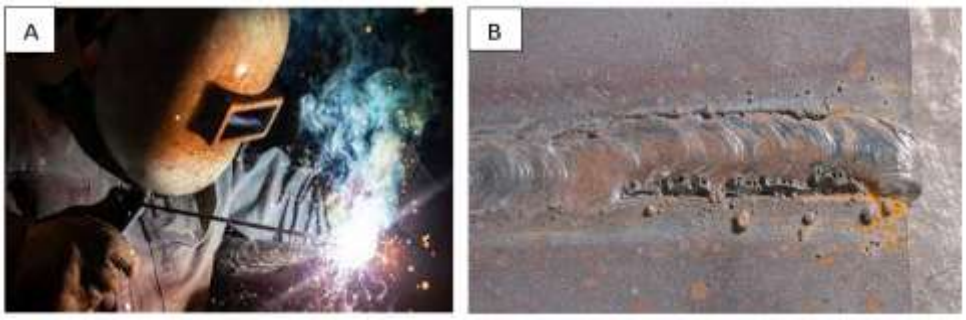

Fig. 1 (A) A TIG welder (www.caller.com) (B) Spatter image (www.twi-global.com)

To achieve the necessary joint quality, process optimization is often necessary (Adin and İşcan, 2022) as algorithms have been utilized to predict and maximize results as regards bonding processes. Ikponmwosa-Eweka and Achebo (2022) used The Response Surface Methodology (RSM) to optimize heat input based on input parameters selected for the welding process. Bucior *et al.* (2022) mathematically represented the relationship between surface roughness parameters and stresses in the surface layer of welded joints that have undergone shot peening. This method can be utilized in practice to control welded joints and select appropriate shot peening process parameters, potentially reducing or avoiding the need for time-consuming and expensive measurements of surface layer stresses. A comprehensive understanding of the keyholing mechanism is crucial for the widespread use of TIG welding in industry. To forecast the temperature field and weld pool geometry during the keyhole welding process, researchers have developed numerous mathematical models (Yan, 2023). The high arc pressure generated during welding can cause depressions in the molten weld pool when high welding currents are used. This can lead to welding flaws such as undercut and humping beads in the weld beads (Delgado-Alvarez et al., 2019). Additionally, the surface layer of the joint is exposed to tensile stresses during this process, which can decrease the fatigue strength of the joint (Li *et al.*, 2018).

MATERIALS AND METHODS

A. Experimental Setup

Sequential pictures were taken by a mobile phone camera that was attached and positioned above and to the side of the welding region, at a distance of 0.7m, to record spatter photos. The vertical and horizontal spatter photos were used to obtain two-dimensional spatter images.

The spatter distribution was determined using the vertically obtained photos, while spatter counting was achieved by using the horizontally captured images. Pictures were taken at 240 frames per second. The brightness of the welding arc caused significant distortion in the collected spatter photos. Therefore, an optical filter was employed to track the welding spatter. The digital lens was fitted with a neutral-density (ND) optical filter, which evenly diffuses incident light across the wavelength spectrum to produce sharper images.

B. Design of Experiment

A design of experiment is a systematic methodology for conducting experiments that can identify cause-and-effect relationships between variables. It is also a structured approach for modifying process inputs and analyzing the corresponding process outputs to quantify both the cause-and-effect relationship and the random variability of the process, while minimizing the number of runs required. Scientific research heavily relies on experimentation, which can be facilitated by software tools such as Minitab and Design Expert. The experimental methodology is employed to gather data and ensure accurate polynomial approximation. Several types of experimental designs are available, including full factorial, Latin hypercube, central composite circumscribed, and central composite face-centered.

C. Identification of Range of Input Parameters

The key parameters considered in this work are welding current, welding voltage, wire diameter, and wire feed speed. The range of the process parameters obtained from literature is shown in the Table-1.

Table-1 Process procedure and their levels

Factors	Unit	Symbol	Low (-1)	High (+1)
Weld Current	Ampere	I	179.9	240.1
Weld Voltage	Volts	V	17.8	23.9
Diameter of wire	Mn	WD	1.20	2.9
Speed of wire feed	Mm/min	WFS	9.9	49.9

D. Materials and Experimental Set-up

The experiment involved welding 100 mild steel coupons, each of size 80 x 40 x 10 (mm), in 20 runs with 5 specimens per run. The plates were beveled and machined before being welded using tungsten inert gas welding equipment. Welding parameters such as current, voltage, wire diameter, and wire feed rates were varied to weld mild steel plates with a thickness of 10 mm. The welding process was shielded with 100% pure Argon gas to prevent air interaction with the weld specimen. The welded specimens were sectioned perpendicular to the welding axis, embedded in resin, and ground using silicon carbide abrasive sheets on a rotating disk, in a five-stage process of 80, 300, 600, 1200, and 4000 grits (Mecatech 334). Subsequently, the specimens were polished using 3µm and 1µm diamond pastes and etched for 45 seconds in a sodium hydroxide solution (1g NaOH + 100 ml H_2O). The macrostructure and microstructure of the samples were examined using a KEYENCE VHX-500F digital microscope. Mild steel plates, 10 mm thick, were utilized to construct the weld samples, which were cut to size using a powered hacksaw. Responses were measured and recorded, edges were ground, surfaces were polished with emery paper, and joints were welded. The weld sample is depicted in the figure below. To detect any phase changes at the cleaned surfaces, SEM was employed to examine the laser-cleaned surfaces in comparison with a reference surface. A Hitachi High Technologies S-3400N Type I, 0.1-30 kV microscope was used for scanning electron microscopy. The spatter collecting setup is shown in Fig. 2.

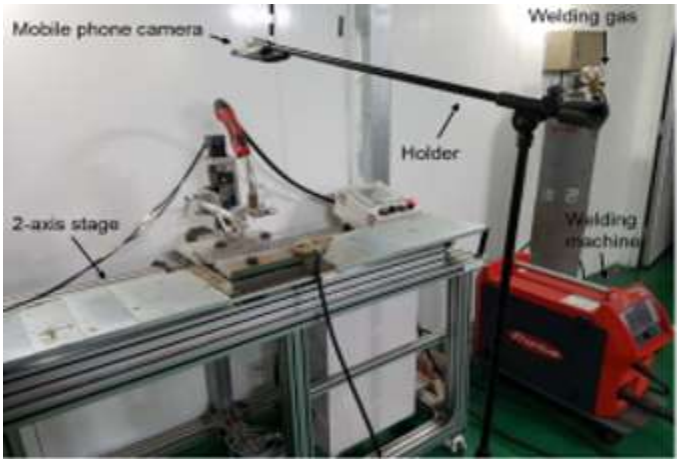

Fig. 2 Spatter collection setup

E. Method of Data Collection

The design expert software was utilized to create a center composite design matrix, resulting in 20 experimental runs. The experimental matrix includes input and output parameters, with the noted responses from the weld samples serving as the data. The number of input parameters is determined by the equation 2n + 2n + k, where k is the number of center points, 2n is the number of axial points, and 2n is the number of factorial points. The data matrix was established based on this formula. The Response Surface Methodology (RSM) and Artificial Neural Network (ANN) were used to analyze the acquired data.

F. Response Surface Methodology

Engineers often use Response Surface Methodology (RSM) to identify the best conditions for a desired process by searching for optimal values of process input parameters that produce the desired outcomes. These optimal values can be either minimum or maximum values for a given function. RSM is a widely used optimization technique for describing the performance of welding processes and identifying the best response. It is a collection of mathematical and statistical techniques that can model and forecast the response of interest, which is influenced by several input variables. RSM is used to optimize the response by predicting the best input conditions for the desired outcomes.

Table-2 Analysis of Variance Components

Variation Source	Degree of Freedom Df	Sum of Squares SS	Mean Square MS	Fisher Ratio F-value
Error of residuals	n-2	$SSE=\sum_{i=1}^{c}\sum_{j=1}^{ni}(y_{ij}-\hat{y}_{ij})^2$	$MSE=\frac{SSE}{n-2}$	
Regression	1	$SSR=\sum_{i=1}^{c}\sum_{j=1}^{ni}(\hat{y}_{ij}-\bar{y})^2$	$MSR=\frac{SSR}{1}$	$F=\frac{MSR}{MSE}$
Lack of fit	C -2	$SSLF_i=\sum_{i=1}^{c}\sum_{j=1}^{ni}(\bar{y}_{ij}-\hat{y}_{ij})^2$	$MSLF=\frac{SSLF}{c-2}$	$F^*=\frac{MSLF}{MSPE}$
Total	n-1	$SSTD=\sum_{i=1}^{c}\sum_{j=1}^{ni}(y_{ij}-\bar{y}_{ij})^2$	-	-

G. Artificial Neural Network

A neural network is a type of processor that is designed to process information in parallel and store it for later use, similar to the human brain. It is often utilized as a data mining tool for uncovering patterns in datasets. The network has two similarities to the brain. Firstly, it can learn from experience through a learning process, and secondly, it can store knowledge through synaptic weights, which represent the strength of connections between neurons. Each neuron receives an input that is weighted by an appropriate value w, and the input to the transfer function f is the sum of the weighted inputs and a bias. The output of the neurons is produced by any differentiable transfer function (f). The multilayer neural network often uses the log-sigmoid transfer function, or logsig, which produces outputs between 0 and 1 as the neuron's net input shifts from negative to positive infinity. Alternatively, the tansig transfer function can be used in multilayer networks. For pattern recognition problems, sigmoid output neurons are commonly used, while linear output neurons are used for other purposes. The artificial neural network is a prediction tool that utilizes a communication approach similar to that of the human brain, which has been programmed into software. It is a data mining tool that analyzes data through processes such as training, learning, validation, and testing.

RESULTS AND DISCUSSION

Two analytical methods were employed to examine the experimental data gathered in this investigation: the response surface methodology (RSM) and the artificial neural network (ANN).

A. Modeling and Optimization using Response Surface Methodology (RSM)

The Response Surface Model (RSM) is a modified version of simple linear regression that includes the second-order effects of non-linear relationships. It is a commonly used optimization approach for identifying the ideal combinations of factors that determine a specific response to an event. RSM is particularly useful in understanding the relationships between multiple predictor factors and several projected responses. The objective of the optimization model was to minimize the splatter index. To achieve this goal, the optimal values for each input variable, including current (Amp), voltage (V), wire diameter, and wire feed speed, were determined to obtain the best possible outcomes for the welding process. To generate data for optimization purposes, the following steps were taken:

i. The statistical design of the experiment was conducted using the central composite design method (CCD). The Design Expert 7.01 software was employed as a statistical tool to facilitate the design and optimization process.
ii. The experimental design matrix consisted of 30 experimental runs, including six center points (k), eight axial points (2n), and sixteen factorial points (2n).

Table-3 presents the sum of squares for the sequential model, which indicates the suitability of the quadratic model in evaluating the experimental data for the splatter index response.

Table-3 Sequential model sum of square for spatter index

	Sum of		Mean	F	p-value	
Source	Squares	df	Square	Value	Prob > F	
Mean vs Total	3.14	1	3.14			
Linear vs Mean	0.45	4	0.11	2.42	0.0747	
2FI vs Linear	0.76	6	0.13	5.91	0.0013	
Quadratic vs 2FI	0.34	4	0.086	20.21	< 0.0001	Suggested
Cubic vs Quadratic	0.041	8	5.185E-003	1.65	0.2615	Aliased
Residual	0.022	7	3.142E-003			
Total	4.75	30	0.16			

Although the cubic polynomial model exhibited a significant lack of fit and was proposed for model analysis, it was observed that the quadratic polynomial model had an insignificant lack of fit. Table-4 demonstrates the model statistics that were computed for the splatter index response using the model terms.

Table-4 Model summary statistics for spatter index

Source	Std. Dev.	R-Squared	Adjusted R-Squared	Predicted R-Squared	PRESS	
Linear	0.22	0.2794	0.1641	-0.0510	1.70	
2FI	0.15	0.7487	0.6164	0.5407	0.74	
Quadratic	0.065	0.9607	0.9240	0.7877	0.34	Suggested
Cubic	0.056	0.9864	0.9435	-0.4913	2.41	Aliased

Table-5 presents the exactness of fit statistics that were utilized to validate the appropriateness of the quadratic model in reducing the spatter index.

Table-5 Goodness of fit statistics for spatter index

Std. Dev.	0.065	R-Squared	0.9607
Mean	0.32	Adj R-Squared	0.9240
C.V. %	20.12	Pred R-Squared	0.7877
PRESS	0.34	Adeq Precision	17.999

Before accepting any model, it is essential to conduct an appropriate statistical analysis. Fig. 5 illustrates the comparison between predicted and actual values for the spatter index to identify any discrepancies or issues in the model's performance. Additionally, a cook's distance plot was constructed to detect any potential outliers in the experimental data for various responses. Fig. 6 displays the calculated cook's distance for the pore size.

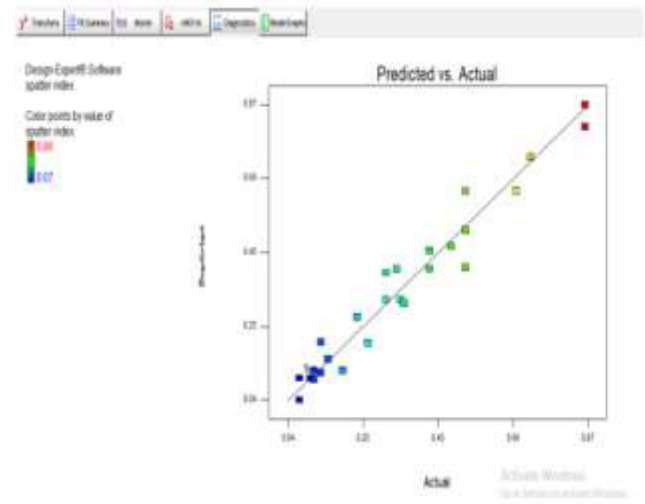

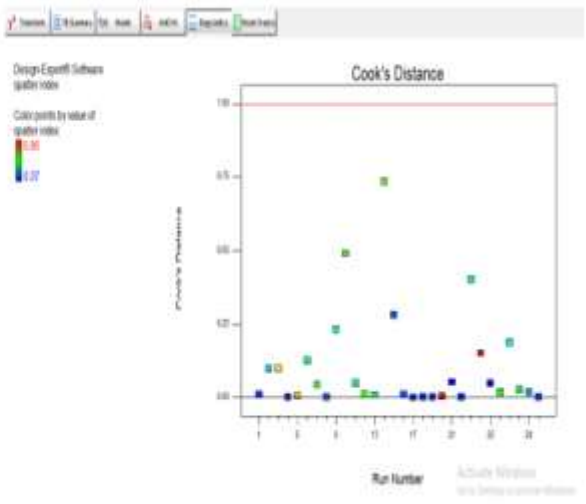

Fig. 5 Plot of Predicted Vs Actual for spatter index

Fig. 6 Cook's distance plot for spatter index

Fig. 7 displays a 3D surface plot used to analyze the impact of multiple input variables on the spatter index, while Fig. 8 depicts 3D surface plots created to study the effect of various input factors on the spatter index.

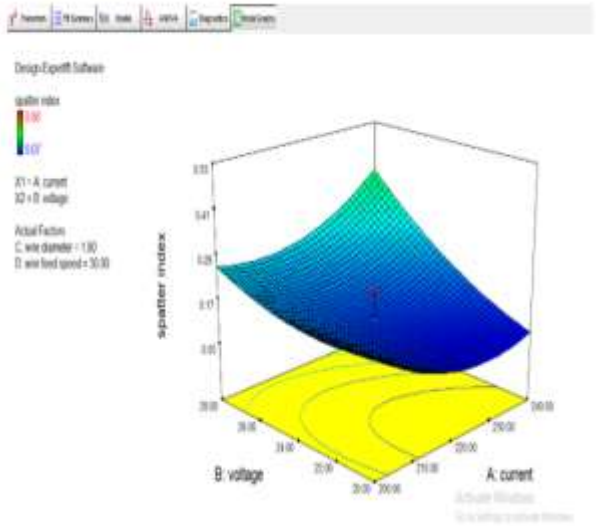

Fig. 7 Effect of current and voltage on spatter index

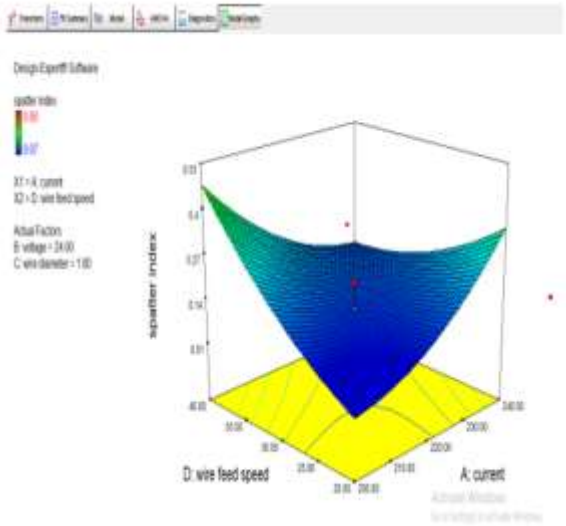

Fig. 8 Effect of wire feed speed and current on spatter index

B. Modeling and Optimization using Artificial Neural Network (ANN)

The selected responses of interest were the spatter index, which were obtained by varying the current, voltage, wire diameter, and wire feed speed. A 4x30 matrix called 'input' contained 30 samples of 4 fixed input variables, while the targets 'Spatter Index' were a 1x30 matrix representing 30 samples of a single output variable. The network architecture and output layer are illustrated in Fig. 9.

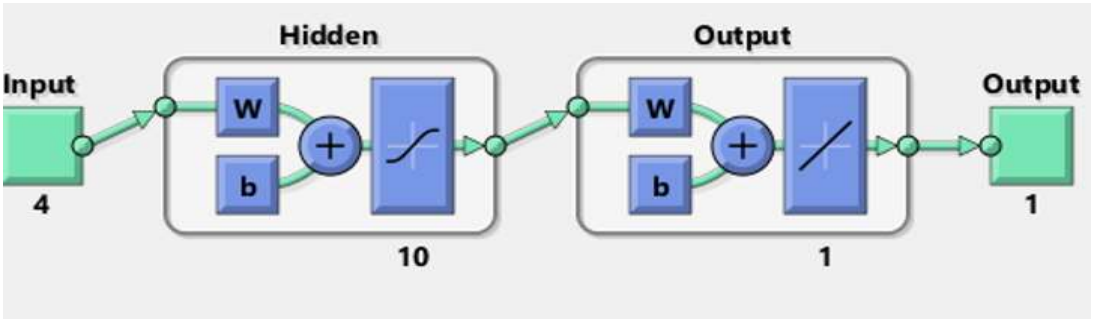

Fig.9 Artificial neural network architecture for predicting spatter index

To ensure the reliability of the results, it is recommended to reserve a portion of the data for validation and testing purposes. In this particular study, the dataset was divided into three distinct groups: training, validation, and testing. Specifically, 70% of the experimental data samples were allocated for training, 15% for validation, and the remaining 15% for testing the performance of the neural network model. This resulted in 20 samples of the entire data used for training while 5 samples each was employed for validation and testing. The Training interphase for the Spatter index: from the result summary, it was noticed that the training of the network model provided a correlation having 99.7% with a mean square error of 1.15E-4. The validation of the network model showed a correlation of 95.9% with a mean square error of 4.64E-3, while testing of the network model resulted in a correlation of 74.4% with a mean square error of 1.14E-2. To gain a better understanding of this, refer to the regression plot of training, validation, and testing for the Spatter index. To evaluate the network learning, a performance plot was created, which is depicted in Fig. 10, indicating that the best validation performance was achieved at epoch 4. The gradient function plot for the spatter index is shown in Fig. 11.

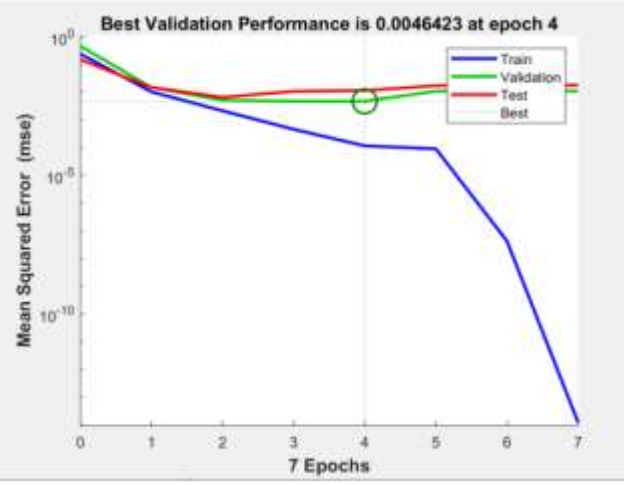

Fig. 10 Performance curve for trained network to predicting Spatter index responses

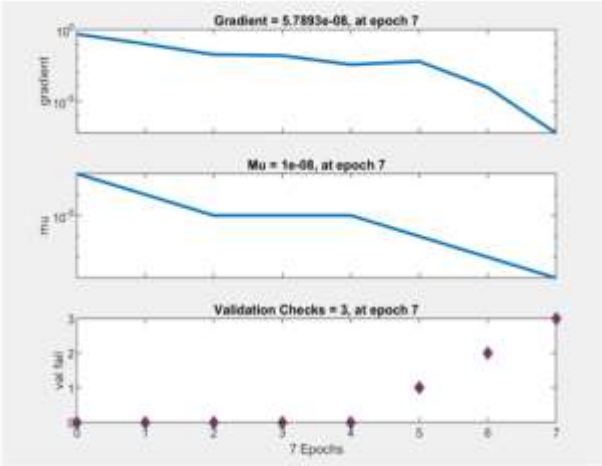

Fig. 11 Neural network gradient plot for predicting Spatter index responses

The regression plot showing the training, validation and testing of the network output is shown in Fig. 12.

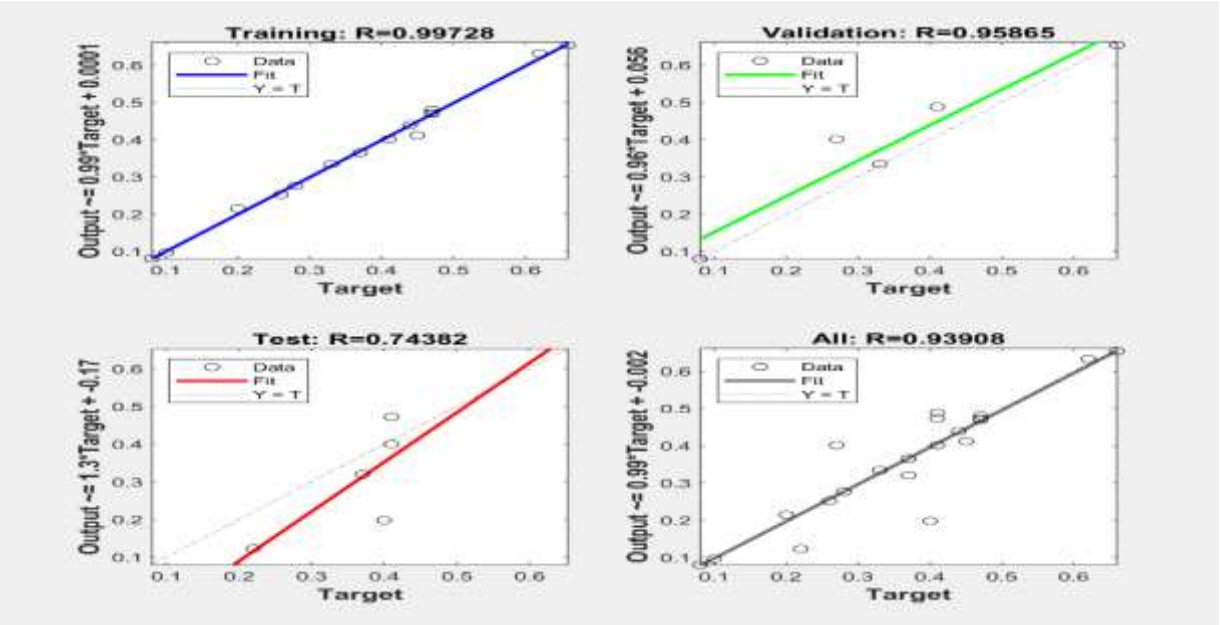

Fig. 12 Regression plot of training, validation and testing for Spatter index responses

C. Comparison between the Experimental values, RSM and ANN Values

A time series plot can help to appreciate the graphical difference between the experimental result and the network output which is shown in Fig. 13.

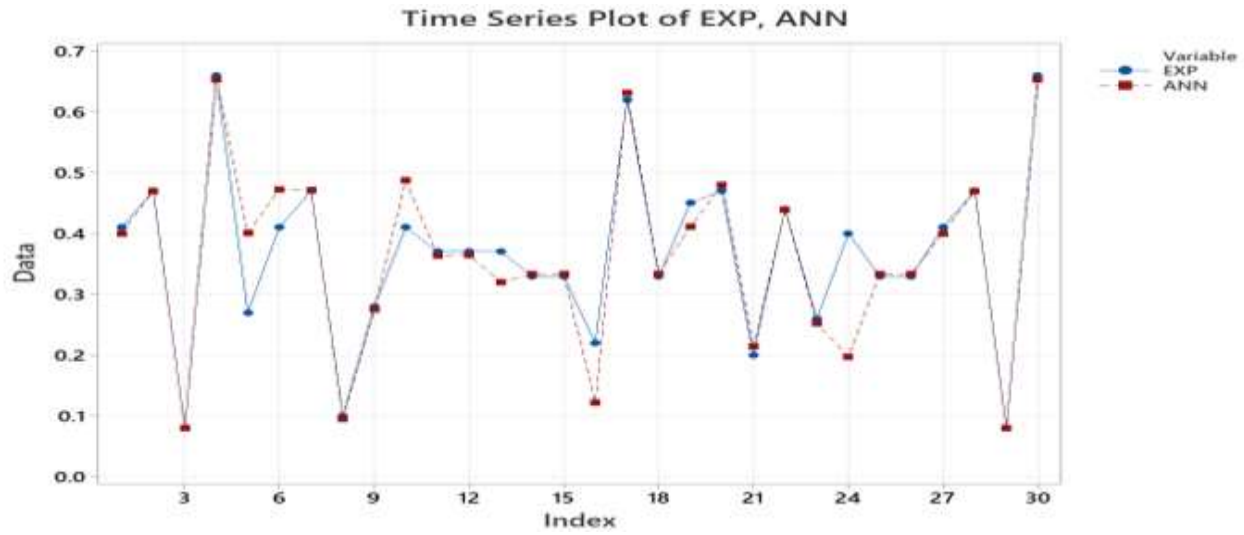

Fig. 13 Time series plot for Spatter index

The regression equation for the Spatter index of exp vs ANN prediction given in equation (1).

EXP = 0.04506 + 0.8875 ANN (1)

The model summary statistics for the network shows the strength of the network output. The result is shown in table 6.

Table-6 Model Summary spatter index

S	R-sq	R-sq(adj)
0.0511320	88.19%	87.76%

The analysis of variance for the network output to check for the significance of the network as shown in table 7

Table-7 Analysis of Variance spatter index

Source	DF	SS	MS	F	P
Regression	1	0.546461	0.546461	209.01	0.000
Error	28	0.073205	0.002614		
Total	29	0.619667			

A fitted plot for the artificial network output was done to illustrate the correlation between the experimental and the spatter index model developed, which is shown in Fig. 14. Two expert approaches, the Response Surface Methodology and the Artificial Neural Network, were utilized in this study to explain the relationship between welding process parameters and the spatter index. The Response Surface Methodology and Artificial Neural Network techniques were used to predict and optimize the welding responses. The input parameters for this process were the current, voltage, wire diameter, and wire feed speed.

The Response Surface methodology was the initial technique utilized, and its results indicate that the behavior of the experimental data is best represented by a second order polynomial model. The significant relationship between the voltage, wire diameter, and electrode density with the spatter index is demonstrated by the quadratic relationship between the process variables, with a p-value of 0.00001. A VIF larger than 10.00 is concerning, but the model's VIF of 1.00 indicates that it is robust.

The model's validity and capability to predict the splatter index were confirmed by the goodness of fit statistics, which yielded a coefficient of determination (R2) of 0.9607.

The model's noise-to-signal ratio was 28.014, indicating a sufficient signal as it is higher than 4. Similar statistical diagnostics were used for the splatter index, resulting in a 96% coefficient of determination. Numerical optimization was eventually achieved, and the Design Expert 7.01 software selected the solution with a desirability value of 0.939 as the best one. The artificial neural network was also used to predict the splatter index. Three sets of input data were randomly generated, with 15% used to verify the network's performance, 70% used for training, and 30% used for testing. The Levenberg-Marquardt algorithm was used for training. During the training phase, the network achieved a correlation value of 99.7% accuracy with a mean square error of 1.15E-4. The network model demonstrated a validation correlation of 95.9% and a mean square error of 4.64E-3. During testing, the network model yielded a correlation of 74.4% and a mean square error of 1.14E-2. The performance plot and correlation plot confirmed that the network had learned correctly and could predict the target outcomes.

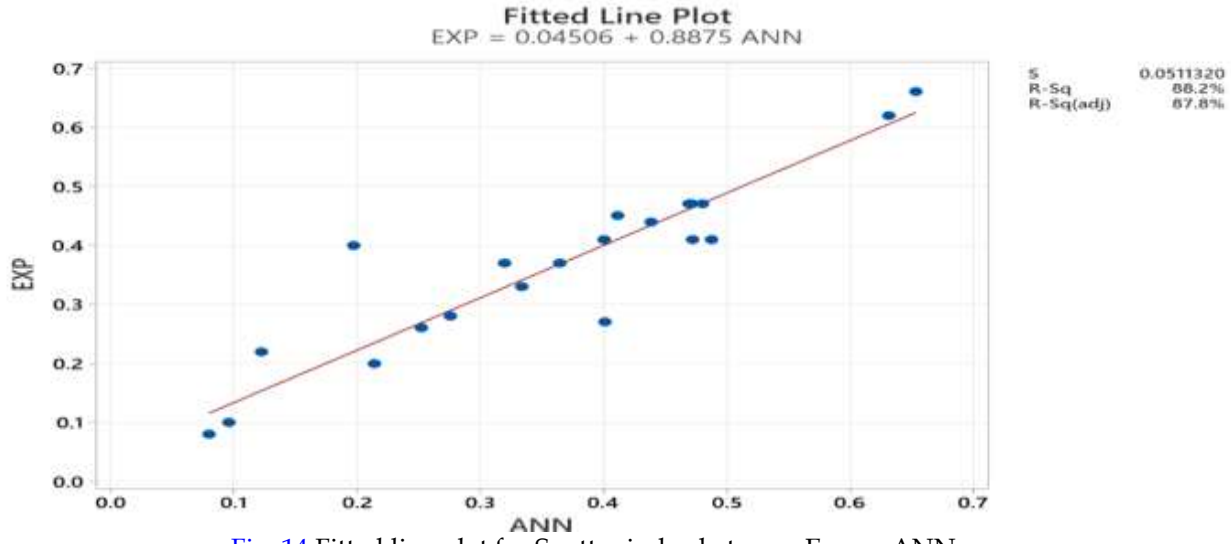

Fig. 14 Fitted line plot for Spatter index between Exp vs ANN

CONCLUSION

In welding, minimizing porosity is crucial for achieving good weld quality and strength. This is because reducing weld flaws and enhancing quality improving responses can determine the overall weld quality. In this study, the response surface approach and artificial neural network model were used to predict and optimize these output parameters. From the results, it is seen that (i) the ANOVA result showed that the lower the current and wire diameter the lower the spatter index of the weld and (ii) the optimal solution of the RSM model is preferred as it is able to predict minimized spatter index. Hence, the response surface methodology is selected as the best optimal solution. The quality of tungsten inert gas welding was improved by employing a well-designed experimental approach utilizing expert systems such as response surface methodology and artificial neural network models. This study optimized welding response; spatter index. The optimal solution will help to produce welds with as little spatter index as possible; thus, the strength, reliability and accuracy of the models have been tested and validated.

CONFLICT OF INTEREST

The authors declare no conflict of interest in the outcome of this research.

REFERENCES

Adin, M.S.; İşcan, B. (2022). Optimization of process parameters of medium carbon steel joints joined by MIG welding using Taguchi method. Eur. Mech. Sci. 6: 17–26

Bhanu V., Gupta A., and Pandey C. (2022). Role of A-TIG process in joining of martensitic and austenitic steels for ultra-supercritical power plants - a state of the art review. Nuclear Engineering and Technology, 54(8): 2755–2770

Bucior M, Kluz R, Trzepieciński T, Jurczak K, Kubit A, Ochał K. (2022): The Effect of Shot Peening on Residual Stress and Surface Roughness of AMS 5504 Stainless Steel Joints Welded Using the TIG Method" *Materials* 15(24), 8835.

Delgado-Álvareza A, Mendez PF, Ramírez-Argáeza MA. (2019) 'Dimensionless representation of the column characteristics and weld pool interactions for a DC argon arc. Sci Technol Weld Join. 1–10

https://www.caller.com/story/news/education/2022

https://www.twi-global.com/technical-knowledge

Ikponmwosa-Eweka O., and Achebo, J.I. (2022). Application of Response Surface Methodology (RSM) TO Optimise the Heat Input During TIG Welding at Steady State Condition. Journal of Energy Technology and Environment Vol. 5(1): 53 – 58

Li, L., Gu, X., Sun, S., Wang, W., Wan, Z., Qian, P. (2018). Effects of welding residual stresses on the vibration fatigue life of a ship's shock absorption support. Ocean. Eng., 170: 237–245

Natrayan L. and Kumar M. (2019)/ Influence of silicon carbide on tribological behaviour of AA2024/Al_2O_3/SiC/Gr hybrid metal matrix squeeze cast composite using Taguchi technique. Materials Research Express, vol. 6, no. (12)

Raja V., Kumar A., Kumari K., Bharanidharan R., Ezhilarasi P., Rajeshkannan S. (2023). Analytical and Neural Network Analysis on Flux-Coated Aluminium Alloy by Activated TIG Welding with Synthesized Nanocomposites, Journal of Nanomaterials, 1-11.

Wang X., Luo Y., D. (2019). Investigation of heat transfer and fluid flow in high current GTA welding by a unified model, International Journal of Thermal Sciences. 142L: 20–29.

Yan Li, Ze Yun, Chen Su, Xiang Zhou, Chuansong Wu (2023). Multiphase and multi-physical simulation of open keyhole plasma arc welding, Case Studies in Thermal Engineering, 41, 102611,

Yogeshwaran S., R. Prabhu, L. Natrayan, and R. Murugan (2015). Mechanical properties of leaf ashes reinforced aluminum alloy metal matrix composites. International Journal of Applied Engineering Research, 10(13): 11048–11052